EUROPEAN ORGANIZATION FOR NUCLEAR RESEARCH
CERN — AB DEPARTMENT

AB-Note-2006-049 RF

A Comparison of π/2-mode standing wave structures for Linac4

R. Wegner, F. Gerigk

Abstract

Cell coupled structures (2 gaps per βλ) at twice the basic frequency provide a higher shunt impedance for proton energies above 90 MeV for Linac4 when compared to drift tube based geometries (1 gap per βλ). For this reason the nominal accelerating structure for the energy range of 90–160 MeV in Linac4 was chosen to be a Side Coupled Structure at 704.4 MHz.
High power klystrons will feed this structure, with the consequence that a large number of cells are coupled together in one module. To provide field stability in a long chain of resonators, a π/2-mode structure will be used. In this report, the three best known and most widely used ones – the Annular Ring Coupled Structure (ACS), the On Axis Coupled Structure (OCS) and the Side Coupled Structure (SCS) – are compared in terms of the electrical parameters Q-value and shunt impedance as well as structure dimensions.

Geneva, Switzerland
18/12/2006

A Comparison of $\pi/2$-mode standing wave structures for Linac4

R. Wegner, F. Gerigk, CERN, Geneva, Switzerland

Abstract

Cell coupled structures (2 gaps per $\beta\lambda$) at twice the basic frequency provide a higher shunt impedance for proton energies above 90 MeV for Linac4 when compared to drift tube based geometries (1 gap per $\beta\lambda$). For this reason the nominal accelerating structure for the energy range of 90–160 MeV in Linac4 was chosen to be a Side Coupled Structure at 704.4 MHz. High power klystrons will feed this structure, with the consequence that a large number of cells are coupled together in one module. To provide field stability in a long chain of resonators, a $\pi/2$-mode structure will be used. In this report, the three best known and most widely used ones – the Annular Ring Coupled Structure (ACS), the On Axis Coupled Structure (OCS) and the Side Coupled Structure (SCS) – are compared in terms of the electrical parameters Q-value and shunt impedance as well as structure dimensions.

1. Introduction

Linac4 [1] is a new H^- linac, currently being developed at CERN to replace the aging proton injector Linac2. At the same time, Linac4 is designed to be the front-end for a future Superconducting Proton Linac (SPL) [2] with a maximum duty cycle of 10%. The high energy section of Linac4 (from 90 MeV to 160 MeV) shall be operated at 704.4 MHz to allow high field gradients and hence a short structure length. Pulsed klystrons with an output power of 4 to 5 MW are foreseen for this section. As the cell dimensions at 704.4 MHz are relatively small, a large number of cells is coupled (about 55 accelerating cells) to allow efficient power distribution from the klystrons to the RF structures. $\pi/2$-mode structures are particularly well suited for this purpose due to their insensitivity (concerning the electromagnetic field distribution in the accelerating cells) to manufacturing errors.

The three best known and widely used $\pi/2$-mode structures, namely the Annular Ring Coupled Structure (ACS), the On Axis Coupled Structure (OCS) and the Side Coupled Structure (SCS) are investigated in detail in this report in order to select the one best suited for Linac4. For this comparison, the electrical parameters (Q-value and effective shunt impedance per length ZT^2 - transit time factor T - as functions of the coupling constant k) as well as the structure dimensions are evaluated. Superfish simulations and stability analysis calculations suggest using coupling constants between 3% and 5% to couple about 55 accelerating cells in one module.

A number of very good reports on $\pi/2$-mode structure comparisons is available [5, 6] as well as detailed reports on the development and the design of each structure type [5, 7, 8, 9, 10, 11, 12]. In this paper, the most recent designs were adapted to 704.4 MHz and investigated in-depth. Starting with 2D simulations (Superfish [3]), each structure was optimised for a beam energy of 90, 130 and 160 MeV respectively. The developed geometries were then modelled and simulated in the 3D simulation package GdfidL [4]. For different coupling slot sizes, the frequencies of both $\pi/2$-modes (with fields either in the accelerating or in the coupling cells) were adjusted to provide a stop band of less than 0.1 MHz and to be within 704.4 ± 0.2 MHz. The electrical parameters Q, Z, ZT^2 were calculated with GdfidL's post processor, whereas the coupling constants were determined by evaluating the resonant frequencies of the 0, $\pi/4$, $\pi/2$, $3\pi/4$ and π-mode.

2. The simulation procedure

In order to simplify the geometry, an infinitely long structure (for each structure type) is modelled by using symmetry planes. Starting with the SCS as the reference, electric and magnetic walls are introduced in the middle of a coupling cell. The basic structure unit then consists of this half coupling cell, one accelerating, one (full) coupling, one accelerating and one half coupling cell. These 5 cells (3 full and 2 half cells) are required to conserve the alternating arrangement of coupling cells for the SCS. (The structures presented in Figures 1 to 3 start with one half accelerating cell. This was done for better visibility of the accelerating mode by cutting a section of a longer structure (9 cells).) The modes with phase advances of $n/4\ \pi$, ($n \in [0, 1, 2, 3, 4]$) are calculated by using electric boundary conditions. The computed $\pi/2$-mode is the one with fields in the coupling cells. In order to simulate the second $\pi/2$-mode (with fields in the accelerating cells), the boundary conditions are changed to magnetic walls. The results of both calculations allow to determine both $\pi/2$-mode frequencies precisely (within the numerical precision and for an infinitely long chain of resonators). Moreover, with the knowledge of the resonance frequencies of the $n/4\ \pi$-modes, it is possible to calculate the coupling factor as well as the next nearest neighbour couplings between accelerating cells and between coupling cells.

For the simulations, a nearly equidistant mesh of 2 mm with fixed mesh lines at critical points (nose positions, cell dimensions, coupling slot positions and widths) was applied. (This results in about 1 million effectively used grid cells for the SCS at 130 MeV). GdfidL's ability to perform these calculations with a parallel algorithm on different computers was employed to reduce the computation time for one calculation to 30 minutes on 4 HP dual RX2600 servers (with Itanium 2 processors at 1.5 GHz and with 2 GB memory – comparable to a 2 GHz Pentium-IV).

Two simulation runs are required to determine both $\pi/2$-mode frequencies (electric, magnetic boundary conditions). The results are used to tune the accelerating and the coupling cells. This procedure is repeated until both frequencies are within 704.4 ± 0.2 MHz and the stop band is less than ± 0.1 MHz. Several iterations (about 4 to 6) were necessary because a change of the dimensions of one cell type has also an (non-linear) effect on the other type due to different meshings.

Each variation of the coupling slot size leads to a change of the resonant frequencies (typically of a few MHz), so that the tuning has to be performed each time in order to provide a similar stop band for all geometries – which is the basis for a trustworthy comparison. For this reason, an automatic tuning algorithm was developed which allows to run several adaptation-simulations per day (and night). Several groups of computers were employed so that 10 different coupling slot dimensions for one particle energy and one structure type could be simulated within 2 to 4 days.

The same method was applied to simulate the ACS and the OCS. In both structures, the coupling slots to the left and to the right of each cell (accelerating as well as coupling) are rotated with respect to each other to reduce higher order couplings (details are described in the sections on the ACS and OCS). Unfortunately, this principle induces a problem for the simulation, as the introduced electric or magnetic walls which are used as boundary conditions, break the arrangement of coupling slots (rotational symmetry / mirror symmetry) for the slots next to this wall. As a result, the calculated $1/4\ \pi$ and $3/4\ \pi$-mode are superpositions of different modes, leading to a mixed field distribution and a considerably reduced resonance frequency. Fortunately, the 0, $\pi/2$ and π-mode are not concerned, they remain nearly unchanged (comparison of structures with 5, 9 and 11 cells). For this reason, the same simulation method as for the SCS was applied, producing reliable results for the coupling factor[1]. Even more important, the electromagnetic field of the accelerating mode (in the accelerating cells) is nearly undisturbed by the broken symmetry in the outer coupling cells, leading to trustworthy results for the electrical parameters Q, Z and ZT^2.

[1]The coupling factor is determined by evaluating the frequencies of the 0, $\pi/2$ and π-modes only. To calculate the next nearest neighbour coupling coefficients, structures with at least 9 cells need to be investigated (pure $1/4\ \pi$ and $3/4\ \pi$-mode). This more than doubles the overall computation time, especially due to the time lost by computer crashes (not related to the GdfidL code). As the higher order coupling factors are not among the most important values for this comparison, it was decided to use models made of 5 cells only.

3. The Annular Ring Coupled Structure (ACS)

The coupling cavities are formed by annular rings in this structure (Figure 1). During early developments [5], severe problems were encountered due to higher order modes in the coupling cells. These modes resonantly couple to the accelerating mode, produce additional losses and hence spoil the electric parameters. Many important improvements have been undertaken since then, resulting in a very compact and well performing geometry for the Japan Proton Accelerator Research Complex (J-PARC). The higher order modes were shifted up in frequency by

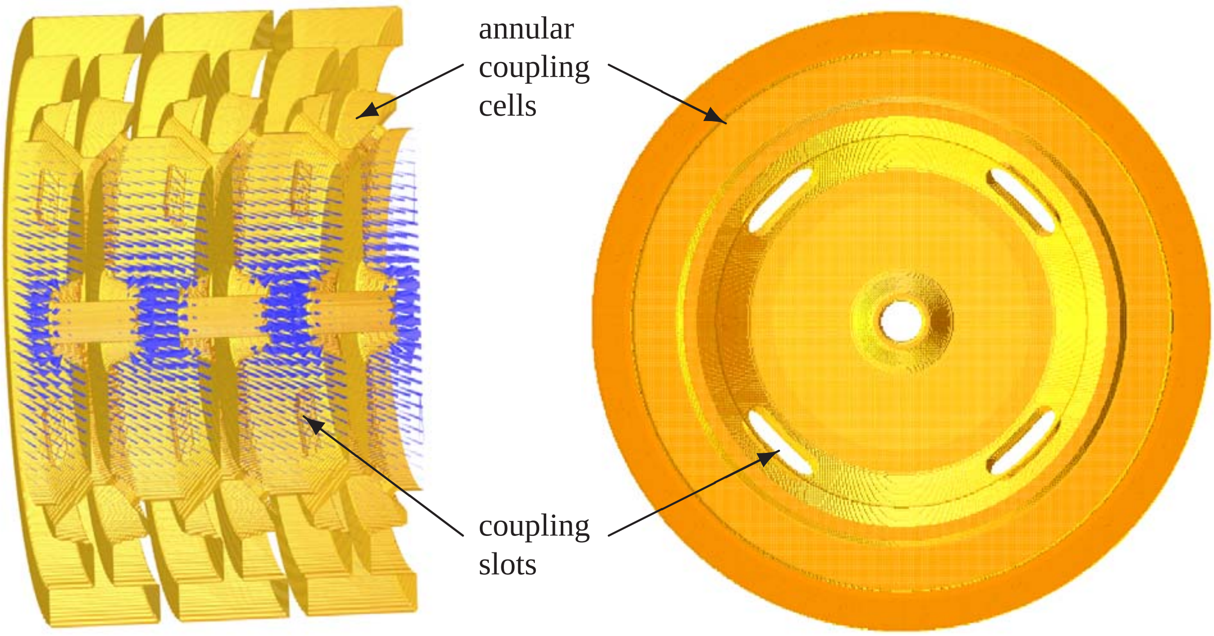

Figure 1: The electric field of the accelerating $\pi/2$-mode in an ACS (left) and a cut through an accelerating cell (right).

reducing the outer radius of the annular rings and by deploying four coupling slots instead of two for coupling accelerating and coupling cells. The slots on the left side of each accelerating cell are rotated by 45° with respect to the ones on the right side to minimise higher order coupling. Moreover, efficient cooling and vacuum systems have been developed, leading to a design that has overcome all initial problems.

After having set up and optimised the structure for particle energies of 90, 130 and 160 MeV, simulations were performed for different coupling slot sizes. The electrical parameters for each energy range are plotted – together with the corresponding curves of the other structures – in Figure 5 to 7. In Table 1, the numbers for a coupling factor of $k = 3\%$ are listed as well as the cell dimensions. The accelerating pass band is located in the range between 694 and 715 MHz and is sufficiently separated from the bands of higher order modes: The TM_{110}-bands are between 753.7 and 754.6 MHz and the TM_{210}-bands are between 869.4 and 871.0 MHz.

Table 1: Simulation results for the ACS at 704.4 MHz for different particle energies. E_0 denotes the (spatial) average electric field on the axis (without transit time).

H^- energy	[MeV]	90	130	160
E_{peak} ($E_0 = 4$ MV/m)	[Kilp.]	0.95	0.88	0.84
$Q(k = 0\%)$		19498	21788	23162
$Q(k = 3\%)$		18624	20727	21960
$Z(k = 3\%)$	[MΩ/m]	39.04	44.70	47.89
$ZT^2(k = 3\%)$	[MΩ/m]	31.12	36.10	38.59
acc. cell length	[cm]	8.55	10.02	10.91
radius of acc. cell	[cm]	13.90	14.20	14.30
radius of coupl. cell	[cm]	23.80	23.40	23.20
transverse inside dimensions	[cm]	48 x 48	47 x 47	46 x 46

4. The On Axis Coupled Structure (OCS)

The coupling cavities of the OCS are on the axis, but they are shortened as much as possible to increase the shunt impedance per total structure length (Fig. 2). To avoid sparking in the coupling cells (in particular during the filling time), a certain minimum length is required [9]. In this case $L_c = 8$ mm was chosen, following a study to upgrade Linac-III at DESY [9, 11]. For a worst case verification, the two $\pi/2$-modes in the designed structure were scaled (in two simulations) in such a way that the same amount of power is dissipated in the accelerating and coupling cell. Comparing the electric peak surface fields, it was found that both levels are nearly identical, validating that sparking is not more likely to occur in the coupling cells than in the accelerating cells during the filling time.

Two different geometries have been investigated, one with cooling channels (septum thickness 15 mm) and one without cooling channels (septum thickness 4 mm). The results are given

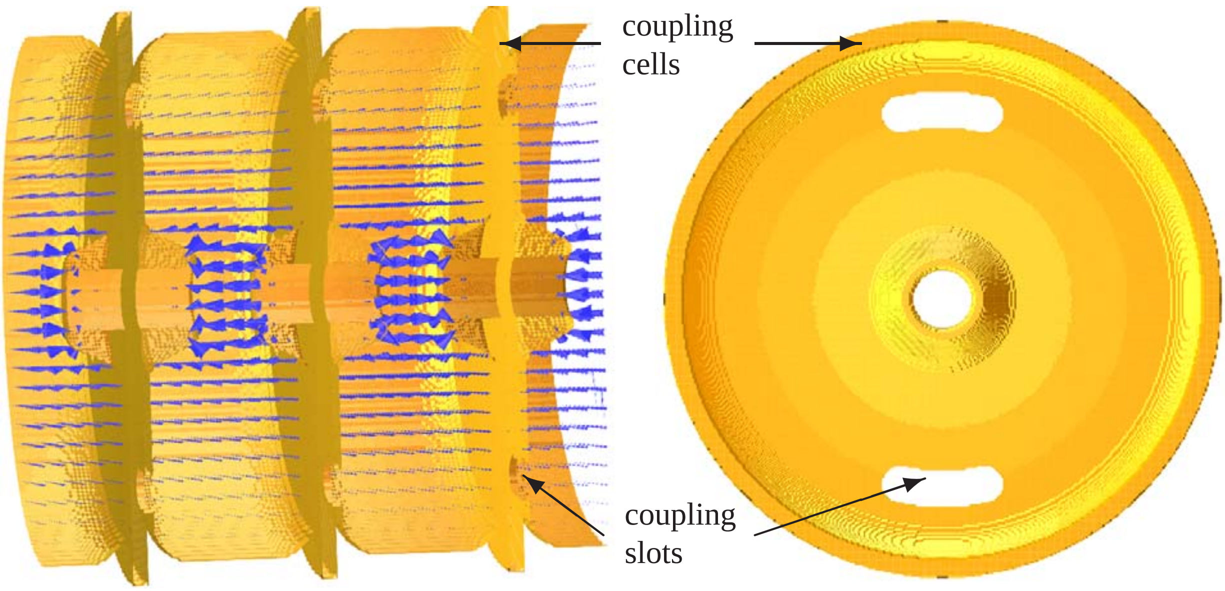

Figure 2: The electric field of the accelerating $\pi/2$-mode in an OCS (left) and a cut through an accelerating cell (right).

in Table 3 and 2, illustrating the severe reduction in shunt impedance for a 22 mm shorter accelerating cell. As a consequence for Linac4, the OCS can only be used efficiently at low duty cycles where no cooling is required. On the other hand, the OCS has proved to be a very compact and reliable structure [10] which allows high coupling coefficients.

As before, simulations for different particle energies and coupling slot sizes have been performed. The results are displayed in Figures 5 to 7 and listed in Table 2. Higher order mode pass bands are well separated from the accelerating pass band (by more than 800 MHz).

Table 2: Simulation results for the OCS at 704.4 MHz **without cooling channels**. The thickness of each septum is 4 mm.

H^- energy	[MeV]	90	130	160
E_{peak} $(E_0 = 4$ MV/m$)$	[Kilp.]	0.96	0.88	0.86
$Q(k = 0\%)$		19010	21444	22614
$Q(k = 3\%)$		18632	20892	22017
$Z(k = 3\%)$	[MΩ/m]	38.80	44.92	47.91
$ZT^2(k = 3\%)$	[MΩ/m]	31.05	36.37	38.82
acc. cell length	[cm]	7.10	8.57	9.46
radius of acc. cell	[cm]	13.83	13.90	13.91
radius of coupl. cell	[cm]	15.83	15.81	15.73
transverse inside dimensions	[cm]	32 x 32	32 x 32	32 x 32

Table 3: Simulation results for the OCS at 704.4 MHz **with cooling channels**. The thickness of each septum is 15 mm.

H^- energy	[MeV]	90	130	160
E_{peak} ($E_0 = 4$ MV/m)	[Kilp.]	1.40	1.20	1.11
$Q(k = 0\%)$		14811	17976	19590
$Z(k = 0\%)$	[MΩ/m]	21.47	28.96	32.97
$ZT^2(k = 0\%)$	[MΩ/m]	17.85	24.56	28.09
acc. cell length	[cm]	4.90	6.37	7.26

5. The Side Coupled Structure (SCS)

The Side Coupled Structure is the nominal accelerating structure for Linac4 [12]. It is well known and has been successfully used in many accelerators (Los Alamos, Fermilab, SNS, etc.). In the SCS, the accelerating cells are connected by coupling cells which are places on the outside, alternating on the top and at the bottom (Fig. 3). The geometry of the coupling cells has been chosen as a compromise between being as small as possible and not causing sparks between the noses. As for the OCS, worst case simulations for the filling time scenario were performed to determine and optimise the electric peak surface field in the coupling cells.

The coupling coefficient is defined by the intersection area between accelerating and coupling cells. In order to avoid sharp edges, the coupling slots are opened by elongated holes with rounded ends and straight parallel sides. It was observed during the investigation, that the losses increase almost linearly with an increase of the coupling factor for small openings.

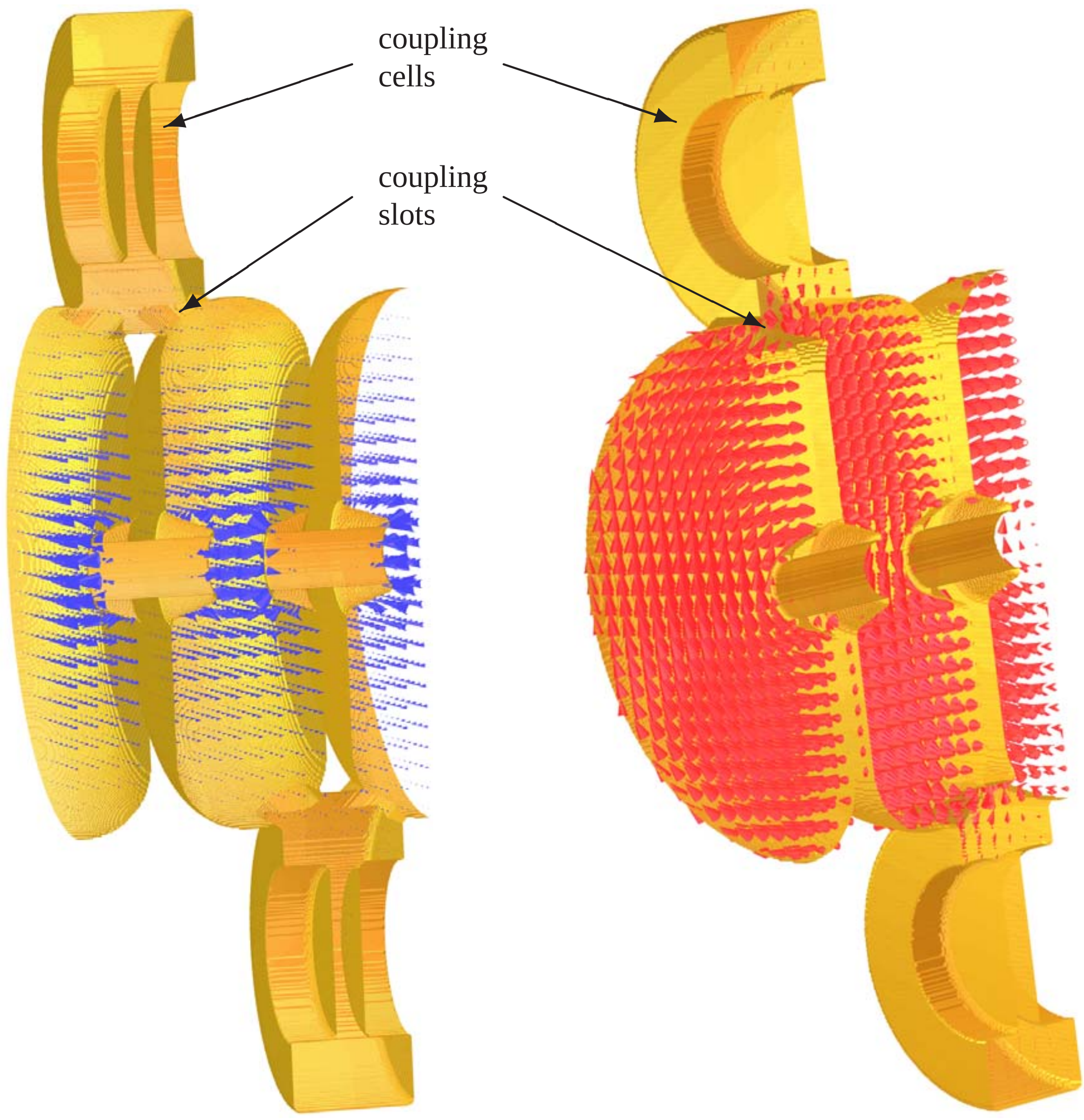

Figure 3: The electric (left) and the magnetic field (right) of the accelerating $\pi/2$-mode in a Side Coupled Structure.

Figure 4: Long coupling slots together with long distances between accelerating and coupling cells (on the right) produce additional edges and therefore an increase of losses.

Beyond a certain value however, this correlation changes and the losses increase stronger than linearly. This effect is caused by very long elongated holes which lead to additional edges at the outside of the coupling cells and hence to the noticed additional losses (Figure 4). To overcome this non-linearity, the overlapping length between accelerating and coupling cells has to be optimised for each coupling coefficient. For this study, three different overlapping lengths were used: 0 mm, 17 mm (optimised for $k = 3\%$) and 22 mm (optimised for $k = 4.5\%$). The simulation results are visualised in Figures 5 to 7 (light green, dashed curves). To obtain an estimation curve for set-ups with optimised overlapping lengths, the linear regimes of the three simulated models were taken and quadratically fitted (dark green curves). For a coupling constant of $k = 3\%$, the details are listed in Table 4. The accelerating band is well separated from pass bands of higher order modes (by more than 600 MHz).

Table 4: Simulation results for the SCS at 704.4 MHz.

H^- energy	[MeV]	90	130	160
E_{peak} ($E_0 = 4$ MV/m)	[Kilp.]	0.95	0.88	0.84
$Q(k = 0\%)$		19533	21965	23376
$Q(k = 3\%)$		19020	21325	22541
$Z(k = 3\%)$	[MΩ/m]	39.72	45.90	49.07
$ZT^2(k = 3\%)$	[MΩ/m]	31.63	37.03	39.48
acc. cell length	[cm]	8.55	10.02	10.91
radius of acc. cell	[cm]	14.35	14.35	14.35
diameter of coupl. cell	[cm]	18.00	18.00	18.00
transverse inside dimensions	[cm]	44 x 29	44 x 29	44 x 29

6. Summary and Conclusions

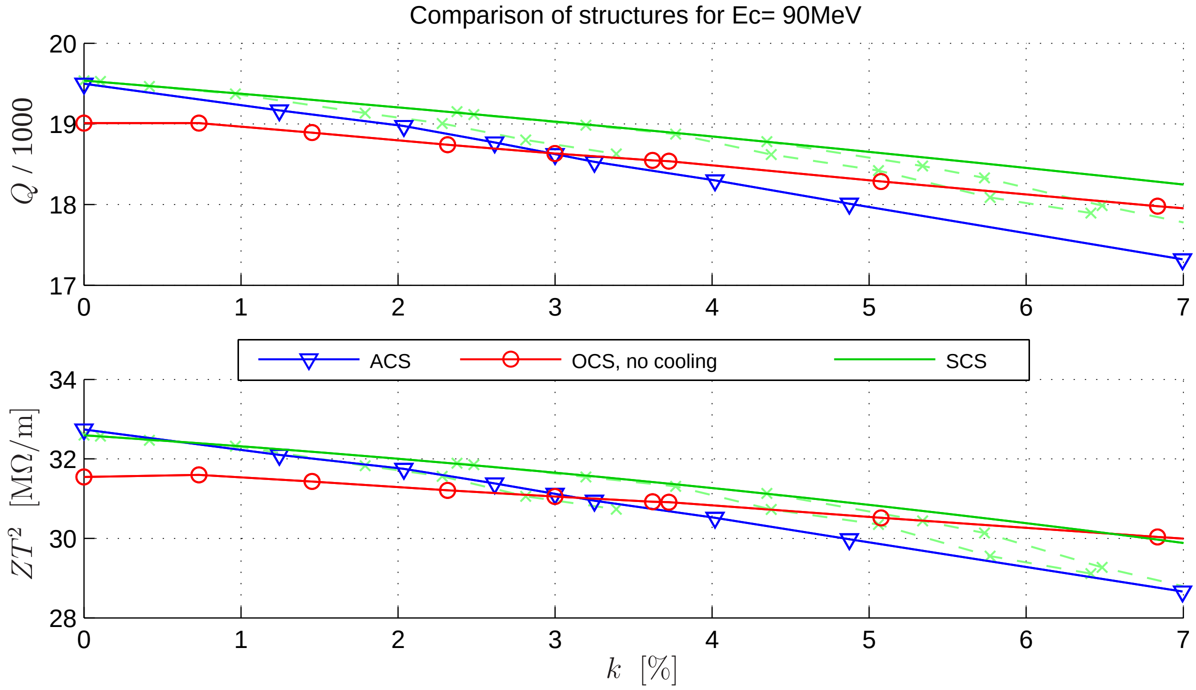

Figure 5: The Q-value Q and the effective shunt impedance per length ZT^2 (with T denoting the transit time factor) as functions of the coupling coefficient k for a particle energy of 90 MeV.

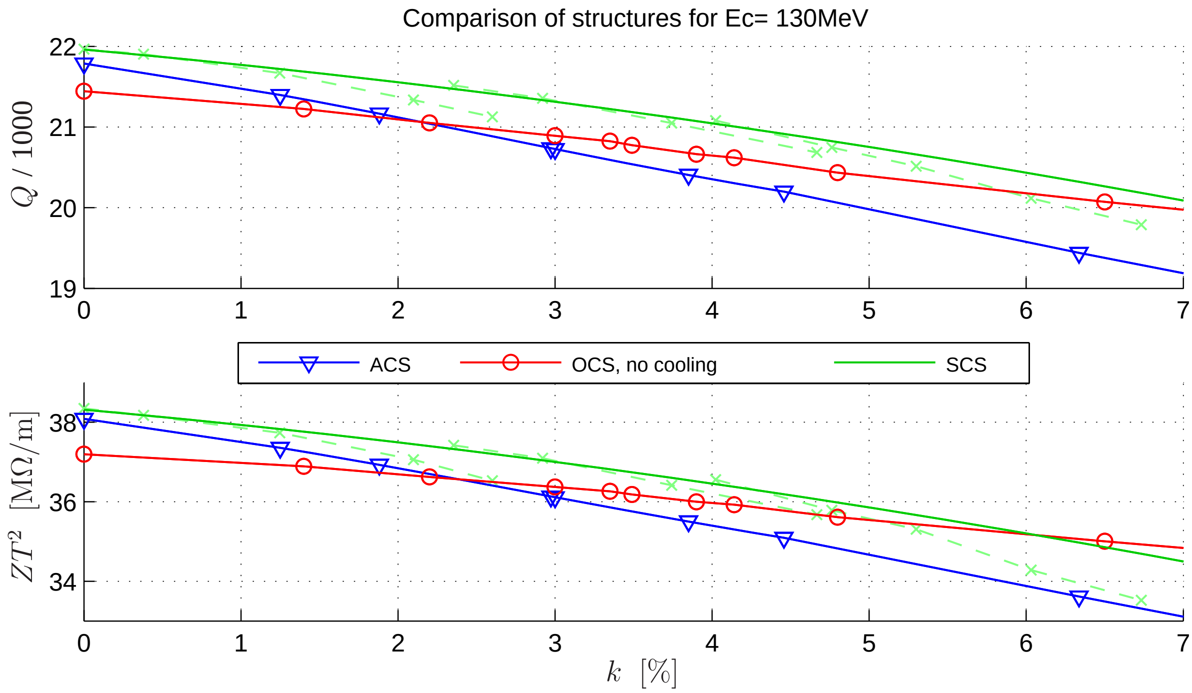

Figure 6: The dependence of Q and ZT^2 on the coupling constant k for a particle energy of 130 MeV.

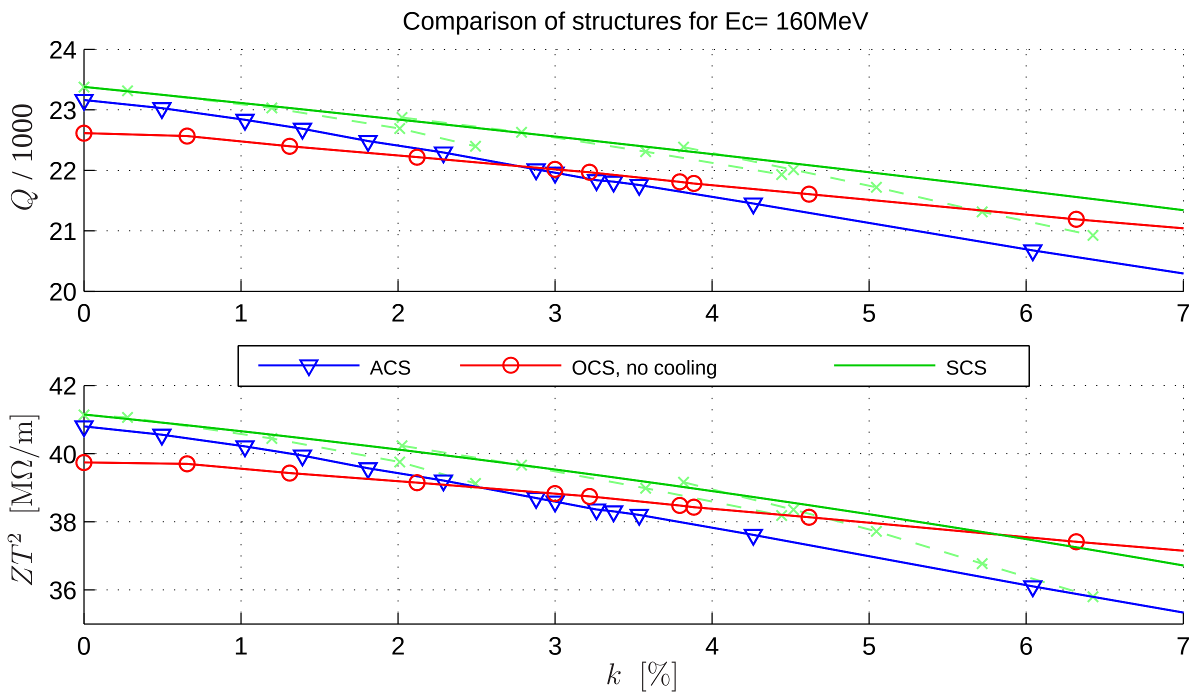

Figure 7: Q and ZT^2 as functions of k for a particle energy of 160 MeV.

The $\pi/2$-mode structures investigated show very similar electrical characteristics (Figures 5-7, Table 5). While the OCS is the smallest in size, it can only be used efficiently at low duty cycles when no cooling is required. To make the upgrade to the Superconducting Proton Linac (duty cycle of about 10%) possible, ACS or SCS structures are mandatory. Both structures are well known and suited for Linac4/SPL.

Although the Q-value and shunt impedance of the ACS and SCS are quite similar, they are better in case of the SCS. The accelerating pass band of the SCS is well separated from the bands of higher order modes. Efficient solutions for cooling and vacuum channels as well as manufacturing procedures and tuning strategies are known for both structures. Comparing the structure dimensions, the SCS is about 40% smaller than the ACS. Considering the present high cost of copper on the international market, a smaller dimension can be an important factor to reduce cost. In conclusion, the SCS is the preferred structure for Linac4.

Table 5: Comparison of the investigated $\pi/2$-mode structures with a coupling factor of 3% for a particle energy of 130 MeV.

		ACS	OCS	SCS
E_{peak}	[Kilp.]	0.88	0.88	0.88
$ZT^2(k=0)$	[MΩ/m]	37.9	37.3	38.1
$\frac{Z_{(k=0)}-Z_{(k)}}{Z_{(k=0)}\cdot k}$ (average)		1.8	0.8	1.4
stop band 1st HOM – acc. band	[MHz]	39	> 800	> 600
transverse inside dimensions	[cm]	47 x 47	32 x 32	44 x 29
cross sectional area	[m^2]	0.22	0.10	0.13

Acknowledgements

We acknowledge the support of the European Community-Research Infrastructure Activity under the FP6 ”Structuring the European Research Area” programme (CARE, contract number RII3-CT-2003-506395)

References

[1] M. Vretenar, N. Alharbi, F. Gerigk, M. Pasini, R. Wegner: *Design and development of RF structures for Linac4*, LINAC06, Knoxville, USA.

[2] F. Gerigk (ed.): *Conceptual Design of the SPL II*, CERN Report 2006-006, Jul. 2006.

[3] *Poisson Superfish*, http://laacg.lanl.gov/laacg/services/download_sf.phtml.

[4] W. Bruns: *The GdfidL Electromagnetic Field Simulator*, http://www.gdfidl.de.

[5] R.K. Cooper, Y. Iwashita, J.M. Potter, S.O. Schriber, D.A. Swenson, J.M. Watson, L.C. Wilkerson, L.M. Young: *Radio-Frequency Structure Development for the Los Alamos/NBS Racetrack Microtron*, Los Alamos National Laboratory document LA-UR-83-95.

[6] V.V. Paramonov: *The coupled cell structures parameters for the large bore hole diameter*, KEK report 2002-5, Aug 2002.

[7] V.V. Paramonov: *The annular coupled structure optimisation for JAERY/KEK joint project for high intensity proton accelerators*, KEK Report 2001-14, Oct 2001.

[8] N. Hayashizaki, H. Ao, K. Hasegawa, Y. Yamazaki, M. Ikegami, T. Kato, V.V. Paramonov: *Structure design of the annular coupled structure linac for the JAERI/KEK joint project*, Proc. of the 2002 Linac Conf., Korea, August 2002.

[9] L.V. Kravchuk, V.V. Paramonov: *The on-axis coupled accelerating structure for application in proton linacs with moderate heat loading*, Proc. of the 1996 Linac Conf., Geneva, August 1996.

[10] H. Euteneuer, A. Jankowiak, M. Negrazus, V.I. Shvedunov: *The 4.9 GHz accelerating structure for MAMI C*, Proc. of the 2000 EPAC, Wien, 2000.

[11] S.K. Esin, L.V. Kravchuk, V.A. Moiseev, P.N. Ostroumov, V.V. Paramonov, W. Ebeling, N. Holtkamp, A. Febel, M. Nagl, J. Maidment: *DESY Linac-III upgrade study*, Proc. of the 1996 Linac Conf., Geneva, August 1996.

[12] E. Benedico Mora, M. Vretenar: *Design of a side-coupled linear accelerator structure for Linac4*, CARE-Note-2005-015-HIPPI.

[13] L.M. Young, J.M. Potter: *CW Side-coupled linac for the Los Alamos/NBS racetrack microtron*, IEEE Trans. Nucl. Sci., Vol. NS-30, No. 4, August 1983.